

Original Article

Supercapacitors for energy storage at high temperature of Cu-Mn-Zn magnetic oxide thin films synthesized by SILAR method

*Dr. Damodar Dattatraya Birajdar ¹

¹Department of Physics, Shri Chhatrapati Sivaji College Omerga, Osmanabad (M.S.), INDIA
damodar.birajdar@gmail.com <https://orcid.org/0000-0003-4414-405X>

*Corresponding Author - damodar.birajdar@gmail.com

DOI – <https://doi.org/10.55083/irjeas.2023.v11i03001>

© 2023 D.D. Birajdar

This is an article under the CC-BY license. This is an open access article distributed under the Creative Commons Attribution License, which permits unrestricted use, distribution, and reproduction in any medium, provided the original work is properly cited.

Abstract: Supercapacitors with their fast charge/discharge efficiency, good cycling life offer remarkable properties as energy storage devices compared to conventional energy storage systems. Cu-Mn-Zn magnetic oxide thin films of composition $\text{Cu}_{0.5}\text{Mn}_{x/2}\text{Zn}_{0.5}\text{Fe}_{2-x/2}\text{O}_4$ ($0.0 < x < 1$) are sintered after being created using the SILAR process. X-ray diffraction, cation distribution, and infrared spectra were examined as structural characteristics. Dielectric characteristics are researched, including the dielectric loss factor and the dielectric constant. The thin films are shown to have spinal structures. As Mn content increases, the lattice constant rises as well. because the polarization of space charges is increasing and as a result, the dielectric characteristics are improving.

Keywords: XRD, Supercapacitors, Thin films, SILAR

1. INTRODUCTION

Because of their quick recharge capabilities, high energy and power densities, extended cycle lives, and safe operation, supercapacitors are the most suited and innovative solution for green energy storage systems. Supercapacitors fill the void left by conventional capacitors and batteries. Global warming, environmental pollution, shortage of fossil fuel and increase in cost of it is economically not good. Because of less availability of nonconventional energy sources, it is necessary to develop safe, green and clean energy sources [1]. Electronic batteries are utilized in electronic

gadgets and automobiles to supply the need for energy [2-4] but due to low power density and maintenance it is not convenient to use. Sodium-ion batteries, Lithium-ion batteries, and supercapacitors has been attracted much attention, because they embrace the great potential in an extensive range of applications [8-10]. Different metal oxides like TiO_2 [11], RuO_2 [12], MnO_2 [13], Fe_2O_3 [14], are extensively studied as electrode materials for pseudocapacitors. Among the transition metal oxides, Ruthenium dioxide (RuO_2) is widely recognized as a highly favorable active material for supercapacitor electrodes. This preference arises from its exceptional

characteristics, including a higher specific capacitance of 2192 F g⁻¹ at a scan rate of 2 mV s⁻¹, excellent electrical conductivity, low equivalent series resistance (ESR), and a broad potential window spanning from 0.0 to 1.0 V [15,16]. The cited sources provide additional information on the specific capacitance, ESR, electrical conductivity, and potential window of RuO₂, thus attributing the information to the respective studies. The usage of thin film technology has transformed the area of electronics, optics, energy storage devices supercapacitors, sensors and magnetism, etc. [17-18]. The SILAR technique was reported for preparation of oxide thin films by Ristov et al. [19]. The capacitance depends on many conditions like method of synthesis, grain size and chemical composition. Ferrite materials are attractive candidates for electrodes in supercapacitors due to their affordability, eco-friendliness, various oxidation states, and abundant availability [20-24]. Ferrites, such as MFe₂O₄ (M = Co, Mn, Ni, Zn, or Mg), are easily synthesized and are ideal for commercial manufacturing on a wide scale. These binary oxides have a large capacitance because redox processes involving two ions take place in them [25]. By sintering the magnetic material under reducing conditions, the valence state undergoes changes, resulting in the formation of individual cations with high conductivity. When such a material is subsequently cooled in an oxygen atmosphere, it is possible to produce a film with high resistivity [26].

2. EXPERIMENTAL

Thin films with general formula Cu_{0.5}Mn_{x/2}Zn_{0.5}Fe_{2-x/2}O₄ (0.0 < x < 1) were prepared by SILAR method using the AR grade compounds Zn(NO₃)₂·6H₂O, Fe(NO₃)₃·9H₂O, Cu(NO₃)₂·6H₂O, Mn(NO₃)₂·4H₂O, H₂C₂O₄·2H₂O as starting materials. Starting ingredients included Zinc nitrate, Manganese nitrate, Copper nitrate, and Ferric nitrate. Without the protection of inert gases, the response technique was used in an environment of air. Metal nitrates and citric acid were assumed to have a 1:3 molar ratio. To create a transparent solution, a modest amount of water that had been double-distilled was used to dissolve the metal nitrates, then ammonia solution was gradually added to preserve the pH. On a hot plate, the combined solution was continuously stirred. The precursor solution was then spun onto the substrate at a speed of 3000 rpm before being calcined. The film thickness was increased by repeating this technique. To create Cu_{0.5}Mn_{x/2}Zn_{0.5}Fe_{2-x/2}O₄ films, the precursor films underwent a post-annealing procedure that took place in a vacuum at 600°C for four hours.

3. RESULT AND DISCUSSION

The XRD patterns are obtained from Regakuminiflex II set up at the angle 2^θ/m in between 20° to 80°. Thin film samples were kept in the cavity for analysis at room temperature.

Cu-Mn-Zn ferrite-related peaks may be seen in the XRD patterns, and there are no additional impurity phases can be seen. The spinel phase's overall crystallinity is increased when Cu is replaced by Mn, and all of the peaks are indexed in accordance with information provided on ASTM cards.

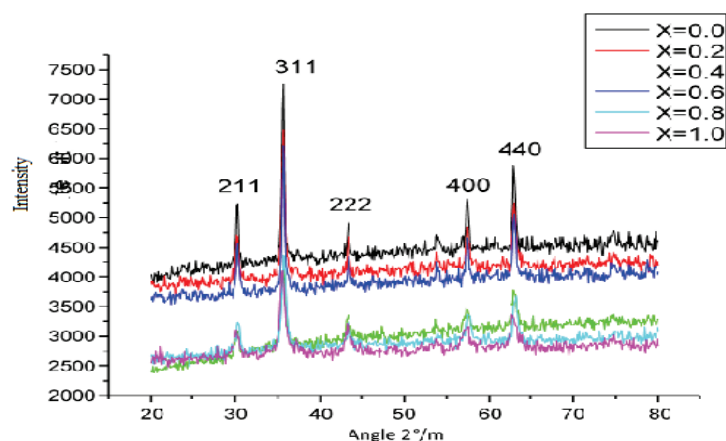


Figure 1. XRD patterns of Cu_{0.5}Mn_{x/2}Zn_{0.5}Fe_{2-x/2}O₄

The XRD patterns for present Mn doped thin films having thickness 1 μm were

analyzed with comparing Cu-Zn thin films. Compared samples shows simple cubic structure

and also increase in 440 peak shows the increase in lattice constant. It shows that the migration of Cu^{2+} ions from octahedral to tetrahedral site. The cation's distribution in the present system was ascertained by looking at X-ray diffraction patterns. The calculated and real intensity ratios were contrasted in this method. The cation distribution in the current investigation is determined using the

Bertaut technique [28]. Using the phrase, this algorithm chooses a few pairs of reflections.

$$\frac{I_{hkl}^{Obs.}}{I_{h'k'l'}^{Obs.}} \propto \frac{I_{hkl}^{Calc.}}{I_{h'k'l'}^{Calc.}} \quad (1)$$

X Composition	d_{AX} A°	d_{BX} A°	Tetra Edge (A°)	Octa Edge (A°)
0	1.907	2,054	3.112	2.821
0.2	1.904	2.050	3.104	2.823
0.4	1.905	2.052	3.123	2.822
0.6	1.908	2.053	3.124	2.828
0.8	1.102	2.055	3.126	2.912
1.0	1.112	2.058	3.128	2.985

Table 1: Tetrahedral and octahedral bonds and edges

Where, $I_{hkl}^{Obs.}$ and $I_{hkl}^{Calc.}$ are respectively, the estimated and measured intensities for reflection (hkl). The literature was used to determine the atomic scattering factor for different ions [29]. The computed cumulative intensity is valid at 0°K, it

should be noted. The reported values were obtained at ambient temperature, therefore in theory, a suitable correction is needed to compare the mean ionic radius (r_A , r_B) of the A and B-sites and x accurately.

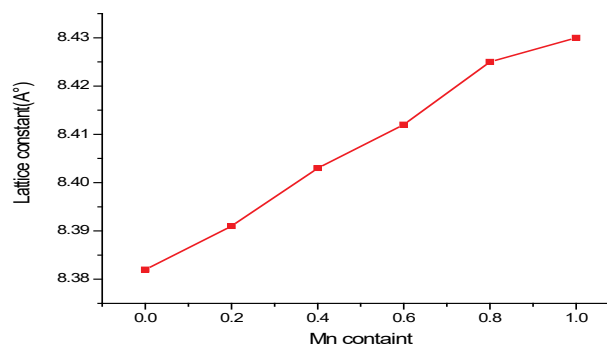


Figure 2. Lattice constant with increasing Mn^{+3} ions.

Dielectric properties of prepared thin films depends on several factors like method of synthesis, Chemical composition etc. The sample mount used for measurement of capacitance and loss is shown in fig.2.

The capacitance bridge can be used for measurement of capacitance and dissipation factor. The dielectric constant of given sample is calculated by given formula i.e.

$$C = (C_o + C_s - C_m) / C_o$$

Where,

C_s - measured capacitance

C_o - geometrical capacitance

C_m - capacitance of sample holder

$$\epsilon'' = \frac{\gamma - \gamma_{\infty}}{\epsilon' \omega} \tag{2}$$

Where, γ_{∞} and γ are DC conductivity and AC conductivity respectively, ϵ' is dielectric constant and ω is frequency.

The approximation of experimental dependence was performed in accordance with equation.

$$\epsilon' = \epsilon'_{\infty} + \frac{\epsilon'_2}{h} \sum_{i=1}^n \frac{P_i D_i}{1 + \left(\frac{f}{f_{ki}}\right)^2} + \frac{\epsilon'_{st} \left[1 + \left(\frac{f}{f_t}\right)^m \cos \frac{m\pi}{2} \right]}{\left[1 + \left(\frac{f}{f_t}\right)^m \cos \frac{m\pi}{2} \right]^2 + \left[\left(\frac{f}{f_t}\right)^m \sin \frac{m\pi}{2} \right]^2} \tag{3}$$

$$\epsilon' = \frac{\epsilon'_2}{h} \sum_{i=1}^n \frac{P_i D_i}{1 + \left(\frac{f}{f_{ki}}\right)^2} \left(\frac{f}{f_{ki}}\right) + \frac{\epsilon'_{st} \left(\frac{f}{f_t}\right)^m \sin \frac{m\pi}{2}}{\left[1 + \left(\frac{f}{f_t}\right)^m \cos \frac{m\pi}{2} \right]^2 + \left[\left(\frac{f}{f_t}\right)^m \sin \frac{m\pi}{2} \right]^2} + \frac{\gamma_{\infty}}{\epsilon_0 \omega} \tag{4}$$

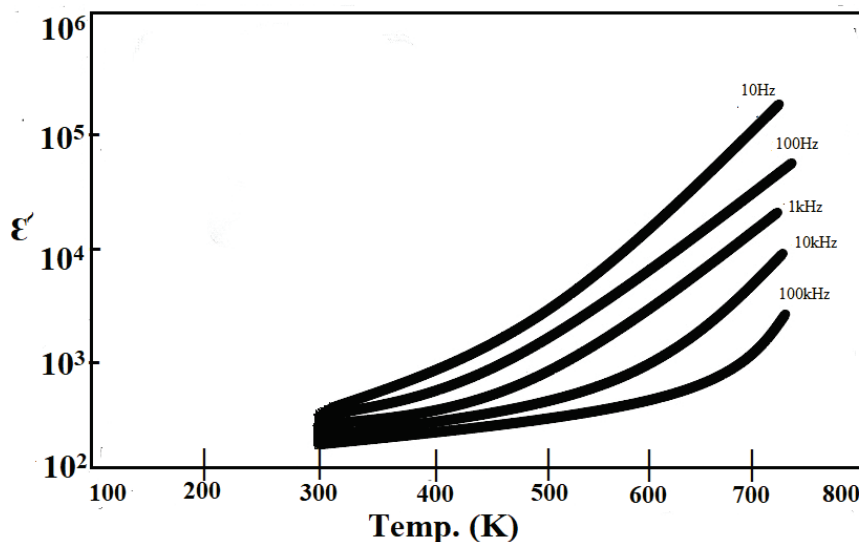


Figure 3. Increase in dielectric constant with temperature

The polarization effect is responsible for the dielectric constant's temperature dependency. The quantity of space-charge carriers controls the polarization of those charges in space. The number of carriers rises as the temperature rises, which enhances the formation of space charge polarization and, as a result, increases the dielectric characteristics.

4. CONCLUSION

This work suggests that high quality Magnetic oxide thin films can be prepared by SILAR method. In supercapacitors, the surface of these materials is crucial. These materials employ redox technology. The material's spinel structure has been verified by X-ray diffraction. The IR spectrum validates the spinel structure and provides details

on the ion distribution between the tetrahedral and octahedral sites. As temperature rises, there are more carriers present, which enhances the build-up of space charge polarization and, as a result, improves the dielectric characteristics.

REFERENCE

1. J. H. Kim, K. H. Lee, L. J. Overzet, G. S. Lee, *Nano Lett.*, 11, (2011).
2. H. Ning, J. H. Pikul, R. Zhang, X. Li, S. Xu, J. Wang, J. A. Rogers, William P. King, and Paul V. Braun "Holographic patterning of highperformance on-chip 3D lithium-ion microbatteries" *Proceedings of the National Academy of Sciences*, vol. 112, no. 21, 6573-6578, 2015, doi: 10.1073/pnas.1423889112
3. N. Nitta, F. Wu, J. T. Lee, and G. Yushin, "Li-ion battery materials: Present and future," *Mater. Today*, vol. 18, no. 5, pp. 252-264, 2015, doi: 10.1016/j.mattod.2014.10.040.
4. H. J. Kim et al., "A comprehensive review of li-ion battery materials and their recycling techniques", vol. 9, no. 7, 1161, 2020, doi: org/10.3390/electronics9071161.
5. D. G. Gromadskyi, J. H. Chae, S. A. Norman, G. Z. Chen, *Appl. Energy*, 159, (2015), 39-50.
6. H. Jung, H. Wang, T. Hu, *J. Power Sources*, 267, (2014), 566-575.
7. S. Maiti, A. Pramanik, S. Chattopadhyay, G. De, S. Mahanty, *J. Colloid Interf. Sci.*, 464, (2016), 73-82.
8. H. Zhou, Y. Zhong, Z. He, L. Zhang, J. Wang, J. Zhang, C. Cao, *J. Alloys Compd.*, 597, 1-7(2014).
9. U. M. Patil, S. B. Kulkarni, V. S. Jamadade, C. D. Lokhande, *J. Alloys Compd.*, 509, (2011).
10. V. J. Mane, D. B. Malavekar, S. B. Ubale, V. C. Lokhande, C. D. Lokhande, *Inorg. Chem. Commun*, 115, (2020).
11. P. M. Kulal, D. P. Dubal, C. D. Lokhande, V. J. Fulari, *J. Alloys Compd.*, 509, (2011).
12. A. D. Jagadale, V. S. Kumbhar, R. N. Bulakhe, C. D. Lokhande, *Energy J.*, 64, (2014).
13. U. M. Patil R. R. Salunkhe, K. V. Gurav, C. D. Lokhande, *Appl. Surf. Sci.*, 255, (2008).
14. S. Jeon, J. H. Jeong, H. Yoo, H. K. Yu, B. H. Kim, M. H. Kim, *ACS Appl. Nano Mater.*, 3, (2020).
15. B. Y. Fugare, B. J. Lokhande, *Mater. Sci. Semicond. Process.*, 71, (2017).
16. X. Cui, Y. Xu, X. Zhang, X. Cheng, S. Gao, H. Zhao, L. Huo, *Sensor Actuat B-Chem*, 247, (2017).
17. G. Brammertz, B. Vermang, H. ElAnzeery, S. Sahayaraj, S. Ranjbar, M. Meuris, J. Poortmans, *Thin Solid Films*, 616, (2016).
18. D. A. Minkov, G. M. Gavrilov, E. Marquez, S. M. Fernandez Ruano, A. V. Stoyanova, *Optik*, 132, (2017).
19. M. Ristov, Gj. Sinadinovski, I. Grozdanov, *Thin Solid Films*, 123, (1985).
20. X. Yao, J. Kong, D. Zhou, C. Zhao, R. Zhou, and X. Lu, "Mesoporous zinc ferrite / graphene composites: Towards ultra-fast and stable anode for lithium-ion batteries," *Carbon*, vol. 79, pp.493-499, 2014, doi: 10.1016/j.carbon.2014.08.007.
21. V. Venkatachalam and R. Jayavel, "Novel Synthesis of Ni-Ferrite (NiFe₂O₄) Electrode Material for Supercapacitor Applications," *AIP Conference Proceedings*, vol. 1665, no. 140016, 2015, doi: 10.1063/1.4918225.
22. P. V. Shinde, N. M. Shinde, R. S. Mane, and K. H. Kim, Chapter 5- Ferrites for Electrochemical Supercapacitors, Editor(s): Rajaram S. Mane, Vijaykumar V. Jadhav, In *Micro and Nano Technologies, Spinel Ferrite Nanostructures for*

Energy Storage Devices, Elsevier, 2020, pages 83-122, ISBN 9780128192375,

doi: org/10.1016/ B978-0-12-819237-5.00005-5.

23. A. Soam, R. Kumar, D. Thatoi, and M. Singh, "Electrochemical Performance

and Working Voltage Optimization of Nickel Ferrite/ Graphene Composite

based Supercapacitor," J. Inorg. Organomet. Polym. Mater., vol. 30, no. 9, pp.

3325-3331, 2020, doi: 10.1007/ s10904-020-01540-7.

24. S. Kuo and N. Wu, "Study on ferrites for supercapacitor application," 56th Annu.

Meet. Int. Soc. Electrochem., no. December, (2015) 1-5.

25. S. F. Shaikh, M. Ubaidullah, R. S. Mane, and A. M. Al-Enizi, Chapter 4- Types,

Synthesis methods and applications of ferrites, Editor(s): Rajaram S. Mane,

Vijaykumar V. Jadhav, In Micro and Nano Technologies, Spinel Ferrite

Nanostructures for Energy Storage Devices, Elsevier, 2020, Pages 51-82, ISBN

9780128192375, doi. org/10.1016/B978-0-12-819237-5.00004-3.

26. C.G. Koops, Phys. Rev., 83, 121.,(1951).

27. L. Weil, E. F. Bertaut, L. Bochirol. J. Phys. Radium, 11, 208, (1950).

28. B.D. Cullity, Introduction to Magnetic Materials, Addison-Wesley,(1972)141.

29. Brabers V A M *Phys. Status Solidi* **33** 563,(1969).

30. Waldron R. D. *Phys. Rev.* **99** 1727,(1955).

31. Hafner S T *Z.Kristallogr.* **115** 331,(1961).

Conflict of Interest Statement: The author declares that there is no conflict of interest regarding the publication of this paper.

Copyright © 2023 D. D. Birajdar. This is an open-access article distributed under the terms of the Creative Commons Attribution License (CC BY). The use, distribution or reproduction in other forums is permitted, provided the original author(s) and the copyright owner(s) are credited and that the original publication in this journal is cited, in accordance with accepted academic practice. No use, distribution or reproduction is permitted which does not comply with these terms.

This is an open access article under the CC-BY license. Know more on licensing on

<https://creativecommons.org/licenses/by/4.0/>



Cite this Article

D.D. Birajdar. Supercapacitors for energy storage at high temperature of Cu-Mn-Zn magnetic oxide thin films synthesized by SILAR method. International Research Journal of Engineering & Applied Sciences (IRJEAS). 11(3), pp. 01-06, 2023. <https://doi.org/10.55083/irjeas.2023.v11i03001>